OPTIMIZATION OF THE FIBER-OPITC FABRY-PEROT INTERFEROMETER CONSTRUCTION

Małgorzata Jędrzejewska-Szczerska, Ryszard Hypszer, Bogdan B. Kosmowski

Department of Optoelectronics and Electronics Systems, Faculty of Electronics, Telecommunications
and Informatics, Gdansk University of Technology, Narutowicza 11/12 Gdańsk 80-233 Poland,
phone: +48 58 347 13 61, fax: +48 58 347 18 48, e-mail: mjedrzej@eti.pg.gda.pl

Abstract − In this article authors present the optimization of fiber-optic Fabry-Perot interferometer to attain the maximum resolution and accuracy of the sensor. The low-finesse Fabry-Perot interferometer working in reflective mode has been implemented. This interferometer was chosen for optimization because using it can have a lot of applications in practice. Its advantages are: relatively simple configuration, potentially low cost, high resolution and low inertia on temperature changes. Furthermore, because of its small size it is possible to make nearly point wise measurement. Authors present theoretical analysis and experimental results of optimization of the fiber-optic Fabry-Perot interferometer, which has been designed and elaborated at our laboratory.

Keywords: Fabry-Perot interferometer, fiber-optic sensor

1. FIBER-OPTIC FABRY-PEROT INTERFEROMETER

One of the common used interferometer is the Fabry-Perot interferometer, which fiber-optic arrangement is shown in figure 1.
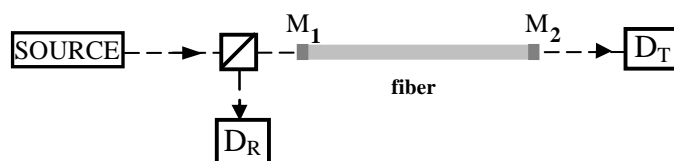

Fig.1. The fiber-optic, Fabry-Perot ineterferometer:
M_1, M_2 – mirrors, D_R – detector in reflection mode,
D_T – detector in transmission mode

This interferometer can work in the reflection or transmission mode. For the reflection mode, the amplitude of the electric vector of the reflected light in the interferometer shown on fig.1, is given by expression [1]:

$$E_i = \frac{(1 - e^{i\varphi})\sqrt{R}}{1 - Re^{i\varphi}} E_0 \qquad (1)$$

where: R – reflectivity of the mirror ($R_1=R_2=R$), φ – the phase difference between interfering beams, E_0 – the amplitude of the electric vector of the incident wave on the first mirror (M_1).

Exemplary, constructions of such an interferometer as a fiber-optic device are shown in figure 2. The interferometer shown in figure 2a is made as a thin film deposited on the end of the fiber. This Fabry-Perot interferometer has two boundary reflective surfaces: fiber/material and material/air [2]. The construction of the Fabry-Perot interferometer, shown in figure 2b, is made by the use of capillary and the reflective plate. When the capillary is filled by the air, the reflective surfaces of this device are made by boundaries: fiber/air and air/reflective plate [3].
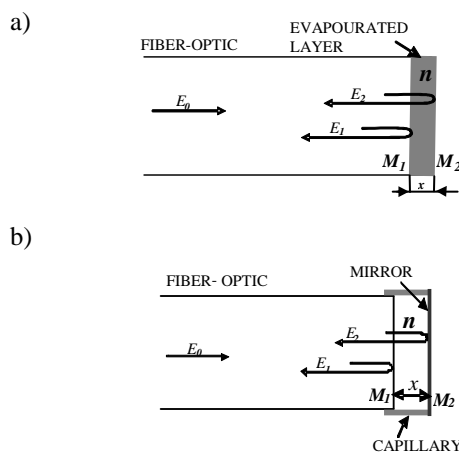
a)

b)

Fig.2. Constructions of fiber-optic Fabry-Perot interferometer: M_1, M_2 – surface with reflection coefficient R_1, R_2; E_1, E_2 – amplitude of wave reflected from the surface *M1, M2*; x – length of the Fabry-Perot cavity; n – refractive index of the Fabry-Perot cavity.

Interferometers shown in figure 2 are a low-finesse Fabry-Perot interferometers working in reflective mode, what help us to obtain relatively high contrast. Taking this into account, amplitudes E_1 and E_2 of waves reflected from the first and the second surface can be describe as follow:

$$E_1 = \sqrt{R_1}\, E_0$$

$$E_2 = (1 - R_1)\,\sqrt{\alpha(x)R_2}\,\exp\left[-\frac{4\pi jnx}{\lambda}\right]E_0 \tag{2}$$

where: E_1, E_2 – amplitude of wave reflected from the surface of reflection coefficient respectively $R1$, $R2$; x – length of the Fabry-Perot cavity, n – refractive index of the Fabry-Perot cavity, $\alpha(x)$ – the attenuation coefficient of the optical intensity due to divergence of light beam in the Fabry-Perot cavity.

Optical intensity at the output of such an interferometer can be expressed by [1]:

$$I_{out} = \left\langle E\, E^* \right\rangle \tag{3}$$

where: $E = E_1 + E_2$; the brackets $\langle\rangle$ – denote time averages; the asterisk $*$ – the complex conjugate.

By substituting from (2), equation (3) can be rewritten as [5]:

$$I_{out}(\nu) = I_c\left[1 + V_0 \cdot \cos(\Delta\varphi(\nu))\right] \tag{4}$$

where: $\quad I_c = I_0\left[R_1 + (1 - R_1)^2 \cdot R_2\alpha(x)\right];$

$I_o = E_o^2$ – intensity of light incident on the first boundary surface of the interferometer, V_0 – visibility of the interference pattern in spectral domain is expressed [4]:

$$V_0 = \frac{2\sqrt{\alpha(x)R_1R_2}\,(1 - R_1)}{R_1 + (1 - R_1)^2\alpha(x)R_2} \tag{5}$$

3. OPTIMIZATION OF THE INTERFEROMETER CONSTRUCTION

In order to attain the best metrological parameters in interferometric sensors the most important task is to maximize the visibility of the measured signal V_0

It can be seen that the maximization of the visibility value of the measured signal V_0 can be done by the optimal choose of the Fabry-Perot interferometer construction. The very important problem is the choose of optical parameters of the material from which the cavity is made. The refractive index of the cavity material influences the value of the reflective coefficients of boundaries. Furthermore, the theoretical investigation shows that one of the critical problem of Fabry-Perot construction is the proper fitting of the geometrical dimension of the cavity, because they influence the attenuation coefficient of the optical signal intensity due to divergence of light beam in the Fabry-Perot cavity. The fiber-optic Fabry-Perot ineterferometers can be made with the use of the multimode or singlemode optic-fiber.

Using a simplified, geometrical model of rays propagation from a multimode fibre into a interferometer cavity, attenuation $\alpha(x)$ of the intensity of the optical signal due to the beam divergence can be calculated. If the thickness of the Fabry-Perot cavity is x, $\alpha(x)$ is expressed as :

$$\alpha(x) = \frac{A^2}{\left[A + 2xtg(\sin^{-1}(NA))\right]^2} \tag{6}$$

where: A – the core radius, NA – the numerical aperture of the fiber.

Sensing interferometer shown in (Fig.2) can also be built using a singlemode fiber. It should be taken into consideration that divergence of light beam occurring on the end of the singlemode fiber is much higher than that on the multimode fiber. This is caused by diffraction effects, which are predominant in singlemode fibers. When the interferometer cavity length x is much larger than the diameter of the fiber core $2A$, only the first-order reflected beam from the end of the fibre and a small part of the first-order reflected beam from the surface will contribute to the interferometric signal. As the mode field diameter is approximated by Gaussian profile then, $\alpha(x)$ of optical signal due to the beam divergence can be calculated by equation [6]

$$\alpha(x) = 1 - \exp\left[-\frac{2\omega_0^2}{\omega^2(x)}\right] \tag{7}$$

where: ω_0 – the mode field diameter, $\omega(x)$ – the mode field diameter at the x distance.

Authors obtained that the visibility reaches the maximum value when:

$$R_2 = \frac{R_1}{(1 - R_1)^2\,\alpha(x)} \tag{8}$$

It can be seen from equation (8) that in order to attain the maximum value of visibility the coefficient R_2 should have very high value ($R_2 \approx 1$). Therefore to the define the value of R_1, which depends on refractive index of the material of interferometer cavity and the fiber, it is possible to estimate from equation (8) the optimal value of the interferometer cavity length.

4. EXPERIMENTS

To verify the theoretical investigation the experimental set-up was designed and built. The system consists of source, an optical processor and the investigated Fabry-Perot interferometer. In low-coherent interferometery, which was used for experiments, it is possible to use time domain or spectral domain signal processing.

When the spectral signal processing is used, the measurement signal can be described as [7]:

$$I_{out}(\nu) = S(\nu)\left[1 + V_0\cos(\Delta\phi(\nu))\right] \tag{8}$$

where: $S(\nu)$ - the spectral distribution of the light source; V_0 - visibility of interference fringes, $\Delta\phi(\nu)$ - the phase difference between interfering beams: $\phi(\nu) = \dfrac{2\pi\nu\delta}{c}$, δ – optical path difference, c – velocity of the light in vacuum.

If the light source exhibits a Gaussian spectrum, the normalized spectra pattern is predicted to be a cosine function modified by the Gaussian visibility profile, as shown in Fig.3.
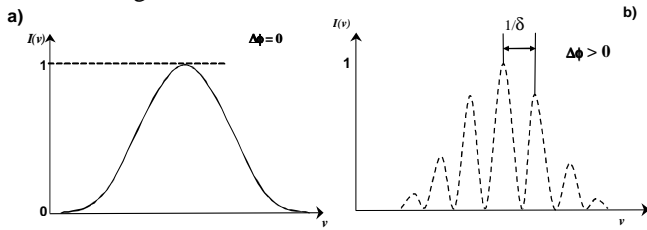

Fig.3. The signal of low-coherence system with spectral signal processing: a) when $\Delta\phi = 0$, b) when $\Delta\phi > 0$. δ − optical path difference

In the spectral domain signal processing the modulation frequency of the measurement signal gives information about the measurand (equation (8)), as shown in Fig.3. It can be noted that for $\Delta\phi=0$ there is no spectral modulation (Fig.3a)). If the phase difference between the interfering beams varies from zero, the function takes the form of the cosine curve (Fig.3b). The spacing of adjacent transmission peak is proportional to the inverse of the optical path difference ($1/\delta$). In this processing, it is necessary to use special measurement equipment and mathematical treatment of the measurement signal.

Authors employed processing of the optical measurement signal in the spectral domain, because of two important advantages. Firstly, such a processing does not need any mechanical elements which established precise displacement. Secondly, it is immune for any change of the optical transmission of the system. The measurement signal $S(\nu)$ processing is based on the channelled spectrum technique. When extrinsic Fabry-Perot interferometer is illuminated by a low-coherent source, the reflection spectrum is modulated by the interference signal from the cavity. [8]

In the experimental set-up is shown in figure 4. In the system as a broadband source a superluminescent diodes with Gaussian spectral density was used (SLD type S1550-G-I-10 with central wavelength $\lambda_0 = 1560$ nm, spectrum width at half maximum $\Delta\lambda=45$ nm, produced by SUPERLUM). As an optical processor the optical spectrum analyzer was implemented (Optical Spectrum Analyzer Ando AQ6319 with wavelength resolution of 1 nm, wavelength accuracy of ±10 pm and close-in dynamic range of 60 dB at peak ±100 pm).
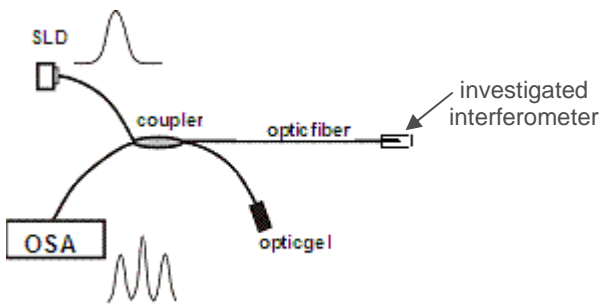

Fig.4. The experimental set-up.

The low-finesse fiber-optic Fabry-Perot interferometer was applied as a sensing head, whose construction is shown in figure 2b. The theoretical investigation proved that the use of singlemode fiber should have been the most efficient. Hence, investigated sensors were made from such a fiber, the silicon capillary and a silver mirror. The interferometer consist of the optic-fiber with uncoated end, which has a reflectance of 0,04. The second reflectance surface is made by the silver mirror with reflectance of 0,99. Therefore, authors got system configuration solution close to optimum. Figures 5a and 5b show the measured signal from the fiber-optic Fabry-Perot interferometer illuminated by the low coherent source.
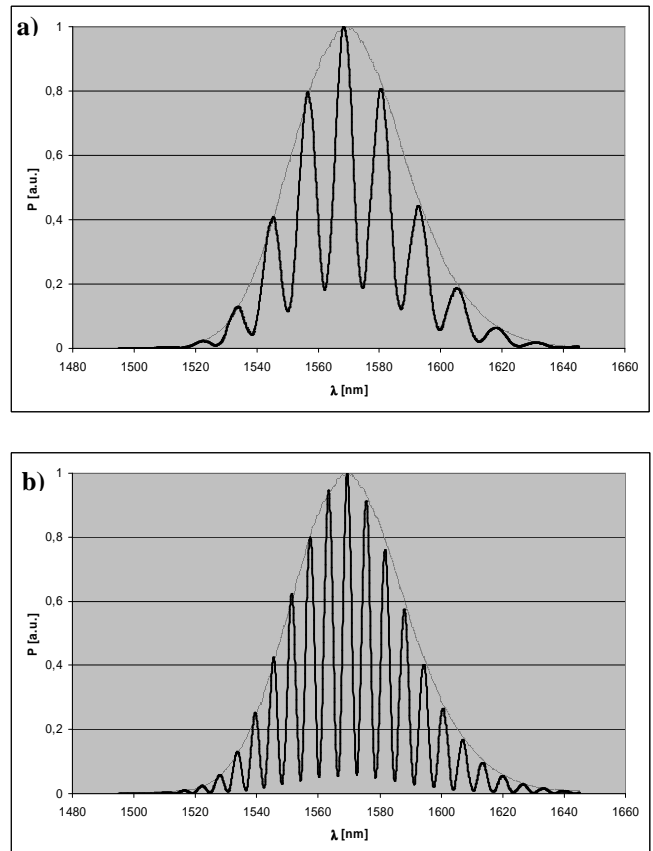

Fig.5. Measured signal from the low-coherent fiber-optic Fabry-Perot interferometer: a) with arbitrarily chosen the length of interferometer cavity; b) with the optimal length of interferometer cavity.

In figure 5a the measured signal form the the low-coherent fiber-optic Fabry-Perot interferometer with the arbitrarily chosen length of interferometer cavity is shown. The signal from the interferometer with the optimal length of the interferometer cavity is presented in figure 5b.

It can be noted that the signal from the interferometer with the optimal construction has bigger difference between the minimum (I_{min}) and maximum (I_{max}) values of the signal than that with the random geometrical dimensions.

For the first interferometer with measured signal shown in figure 5a, the visibility is: $V_0 = 0,67$ and for the second, which measured signal is shown in figure 5b, the visibility has value: $V_0 = 0,99$.

These difference in values of visibility confirmed us that by the optimal selection of the geometrical dimension of the Fabry-Perot cavity it is possible to optimized its metrological parameters by optimizing the contrast of the measured signal.

4. CONCLUSIONS

In this work the method of optimization of the fiber-optic, Fabry-Perot interferometer construction has been presented. The low-finesse Fabry-Perot interferometer working in reflective mode has been investigated. This interferometer was chosen for optimization because of broad range of it potential applications. Its advantages are: relatively simple configuration, potentially low cost, high resolution and low thermal inertia. Furthermore, because of its small size it is possible to make nearly point wise measurement.

Theoretically and experimentally has been investigated the use of the multimode fiber and the singlemode fiber in Fabry-Perot sensor. The suitable construction was investigated in order to maximize fringe visibility.

Presented preliminary results can be the base for building fiber-optic sensor of physical quantities.

REFERENCES

[1] M.Born , E. Wolf *Principles of Optics*, Pergamon Press, Oxford, 1993.

[2] M. Jędrzejewska-Szczerska, R.Bogdanowicza, M.Gnyba, R.Hypszer, B.Kosmowski, " Fiber-optic temperature sensor using low-coherence interferometry", *The European Physical Journal – ST*, vol.154, pp.107-112, 2008

[3] F.Yu [ed]: *Fiber Optic Sensors*, Marcel Dekker, New York, 2002

[4] T.Liu, D.Brooks, A.Martin, R.Badcocko, G.Fernando, "Design, fabrication and evalution of an optical fiber sensor for tensile&compressive strain measurements via the use of white light interferometry", *Proc. SPIE*, vol.2718, pp.408-416, 1996

[5] S.Egorov , A.Mamaev , I.Likhachiev, " High reliable, self calibrated signal processing method for interferometric fiber-optic sensors", *Proc. SPIE*, vol.2594, pp.193-197, 1996

[6] Bing Yu, Dae Woong Kim, Jiangdong Deng, Hai Xiao, Anbo Wang, "Fiber Fabry-Perot sensors for detection of partial discharge in power transformers", *Applied Optics*, vol.42, pp.3241-3250, 2003

[7] S.Egorov, A.Mamaev, I.Likhachiev, "Spectrally encoded fiber-optic sensors based on Fabry-Perot interferometer", *Proc. of SPIE*, vol.1972, pp.362-369, 1999

[8] Shaoji Jiang, Bin Zeng, Youcheng Liang, Baojun Li, "Opical fiber sensor for tensile and compressive strain measurements by with-light Fabry-Perot interferometry", *Optical Engineering* vol.46, pp.034402-1÷5, 2007